CHAPTER 3. TOXICOKINETICS, SUSCEPTIBLE POPULATIONS, BIOMARKERS, CHEMICAL INTERACTIONS

3.1 TOXICOKINETICS

Aldehydes, including acrolein, are generated via endogenous processes (Burcham 2017). Acrolein can be produced endogenously by the following processes: (1) oxidation of methionine followed by Strecker degradation to methional sulfoxide, which can then decompose forming acrolein; (2) myeloperoxidase-catalyzed oxidation of threonine; (3) oxidation of cell function-regulating polyamines (spermine and spermidine); and (4) lipid peroxidation (Burcham 2017). The primary process producing endogenous acrolein is believed to be lipid peroxidation, in which unsaturated lipids undergo autocatalytic degradation (oxidation followed by beta cleavage of alkoxyl radical to form acrolein and other electrophiles) (Burcham 2017). Endogenous production of acrolein complicates the interpretation of toxicokinetic studies of acrolein, particularly in humans.

Human studies of acrolein with information on absorption, distribution, metabolism, and excretion are limited. Acrolein toxicokinetics have been studied in a small number of studies in dogs and rodents, with most quantitative data derived from studies conducted in rodents. An overview of these data is presented below.

- Studies in animals indicate that acrolein is absorbed in the respiratory tract, primarily the upper respiratory tract, following inhalation exposure. Human and animal studies demonstrate that acrolein is absorbed from the gastrointestinal tract following oral exposure.

- Animal studies indicate distribution of acrolein after inhalation and oral exposure is limited due to the strong reactivity of acrolein with tissues at the exposure site. Acrolein is a highly reactive electrophile that reacts readily with sulfhydryl groups from proteins and amino acids.

- The main metabolic pathway is through acrolein conjugation with reduced glutathione (GSH) followed by enzyme-catalyzed conversion to mercapturic acid products for urinary excretion. The major urinary products of this pathway are 3-HPMA and CEMA. Minor metabolic pathways are postulated to yield glyceraldehyde and malonic acid.

- Acrolein is not excreted unchanged. Acrolein metabolites are excreted primarily in the urine and exhaled air following oral or inhalation exposure; small quantities are excreted in feces.

3.1.1 Absorption

No studies were located regarding the rate and extent of absorption in humans after inhalation exposure to acrolein. The collection of such data would be problematic, as acrolein is highly reactive with any nucleophilic binding site that it encounters during exposure by any route.

Animal data demonstrate that inhalation absorption of acrolein occurs readily at local sites. Struve et al. (2008) isolated the upper respiratory tract of anesthetized rats to measure the uptake of inhaled acrolein in this region (percent difference between concentration in air before entering the rat nose and the concentration exiting the trachea). At acrolein concentrations of 0.6–3.6 ppm for up to 80 minutes and a constant (unidirectional) airflow rate of 100 mL/minute, uptake efficiency estimates declined with exposure concentration from >90% at 0.6 ppm to ~55% at 3.6 ppm. After the airflow rate was increased from 100 to 300 mL/minute, small decreases in uptake efficiency were seen, with the same concentration-related decrease (85% at 0.6 ppm to 35% at 3.6 ppm) (Struve et al. 2008). When measured over time, efficiency of uptake at 3.6 ppm exposure decreased for the first 12–24 minutes and then remained relatively constant over the remainder of the 80-minute exposure period (Struve et al. 2008). Pre-exposure to acrolein resulted in higher uptake efficiency in the upper respiratory tract: groups of rats pre-exposed to 0.6 or 1.8 ppm acrolein for 6 hours/day, 5 days/week for 14 days had higher uptake efficiency than naïve counterparts (Struve et al. 2008). These experiments demonstrated that at low ppm concentrations, the upper respiratory tract efficiently removes a substantial portion of inhaled acrolein before it reaches the lower respiratory tract, and that higher exposure concentrations lead to greater exposures to the lower respiratory tract. Similar results were obtained in an earlier study in rats using a comparable design (Morris 1996); absorption in the upper respiratory tract of rats did not reach steady state in 40 minutes and was found to be inversely correlated with concentration and respiration rate. Likewise, when the isolated upper respiratory tract of mice was exposed to 1.1 ppm acrolein at a flow rate of 25 mL/minute, the uptake efficiency was estimated to be >92% (Morris et al. 2003). In anesthetized mongrel dogs exposed to concentrations of 172–262 ppm acrolein for 1–3 minutes, retention was independent of the respiratory rate (Egle 1972). At ventilation rates of 6–20 respirations/minute, 80–85% of the inhaled acrolein was retained in the entire respiratory tract, with 75–80% localized in the upper respiratory tract.

While no studies were located of absorption in humans after measured oral doses of acrolein, acrolein absorption was demonstrated in 19 humans by analysis of the urinary metabolite, 3-HPMA; the serum acrolein-protein conjugate [Nε-(3-formyl-3,4-dehydropiperidino)lysine (Acr-FDP)]; and buccal cell

acrolein DNA adducts [α- and γhydroxy-1,N2-cyclic propano-2′-deoxyguanosine (α-OH-Acr-dG and γ-OH-Acr-dG)] up to 24 hours following ingestion of fried fast foods (Wang et al. 2019). Levels of urinary 3-HPMA increased after fast food consumption and generally peaked 12 hours post ingestion; thereafter, the concentrations began decreasing, reaching near-baseline concentrations after 24 hours. At all timepoints after exposure, buccal cell acrolein DNA adducts were increased, while serum protein adducts were unchanged from pre-exposure levels (Wang et al. 2019).

Parent et al. (1996a) administered gavage doses of 2.5 or 15 mg/kg [2,3-^{14}C] acrolein to male and female Sprague-Dawley rats. Doses of 2.5 mg/kg were extensively absorbed, as only 12–15% of the initial dose was found in the feces. In the high-dose group, 28–31% of the initial dose was found in the feces.

No studies were located regarding absorption of acrolein in humans after dermal exposure. In cases of accidental dermal exposure, effects were restricted to the exposed region of the body, presumably because of the high reactivity of acrolein. In an *in vitro* study of dermal permeation, human dermis was exposed to acrolein vapor (153 ppm) in static Franz diffusion cells exposing a surface area of 0.64 cm^2 for up to 30 minutes (Thredgold et al. 2020). Estimates of dermal penetration (measured by analysis of receptor fluid) and absorption (measured by analysis of skin tissue after exposure) were negligible (0.480 and 0.887 μg/cm^2, respectively).

Limited information is available regarding dermal absorption of acrolein in animals. The percutaneous LD_{50} for rabbits ranged from 160 to 1,000 mg/kg, depending on the acrolein concentration and vehicle (water or mineral spirits) (Albin 1962). LD_{50} values for acrolein administered in mineral spirits are lower than those in which water served as the vehicle, likely because of the greater skin permeability of mineral spirits.

3.1.2 Distribution

Acrolein is highly reactive electrophile. Because it readily reacts with biological nucleophiles (proteins, DNA, glutathione), distribution is primarily local at the site of entry with limited systemic distribution.

No studies were located regarding distribution of acrolein in humans or animals after inhalation exposure. Studies regarding absorption in animals exposed by inhalation demonstrated uptake in respiratory tract tissues, but did not indicate whether systemic distribution occurred (Egle 1972; Morris 1996; Morris et al.

2003; Struve et al. 2008). Urinary metabolites of acrolein were detected in mice exposed to 0.5–1 ppm acrolein for 6 hours, suggesting that systemic absorption occurred (Conklin et al. 2017b).

No studies were located regarding distribution of acrolein in humans after oral exposure; however, following voluntary ingestion of fried fast food, the increased concentration of the acrolein urinary metabolite, 3-HPMA, suggested some systemic distribution, while increased acrolein DNA adducts in buccal cells indicated local distribution in the oral cavity (Wang et al. 2019).

In a study conducted by Draminski et al. (1983), the acrolein conjugated metabolite, S-carboxyethyl-mercapturic acid, was identified in the urine of rats after oral administration of a single dose of 10 mg/kg of acrolein, suggesting distribution of acrolein to the liver and kidney, where conjugation most likely occurred. Parent et al. (1996a) detected radioactivity in the kidney, spleen, lungs, blood, liver, fat, adrenals, and ovaries at similar levels in rats sacrificed 168 hours after oral administration of 2.5 mg/kg [2,3-^{14}C]acrolein. Radioactivity in blood and tissue represented approximately 1% of the dose, indicating limited systemic distribution. After i.v. administration of the same dose, radioactivity levels in the kidneys, spleen, lungs, blood, and adrenal glands were between 2- and 100-fold higher compared with oral administration (Parent et al. 1996a).

No studies were located regarding distribution of acrolein in humans or animals after dermal exposure.

3.1.3 Metabolism

Acrolein metabolism is attributed to conjugation reactions. The primary reaction involves the electrophilic site of acrolein reacting directly with the cysteinyl thiol (-SH) of proteins (lysine and histidine) and nonproteins (glutathione), and this reaction may be nonenzymatic or catalyzed by glutathione-S-transferase (Esterbauer et al. 1975; Parent et al. 1998). In experiments in non-biological, cell-free systems, acrolein formed thiol ethers rapidly (within seconds) in reactions with glutathione or cysteine (Esterbauer et al. 1975, 1976). In *in vitro* experiments using cultured human bronchial cells, human mucoepidermoid pulmonary carcinoma cells, and isolated cell preparations from rat liver and kidneys, acrolein formed conjugates with glutathione and/or thioredoxin and with amino acids including lysine, histidine, cysteine, and N-acetylcysteine (Dawson et al. 1984; Dupbukt et al. 1987; Gurtoo et al. 1981; Xiong et al. 2021, Yang et al. 2004; Zitting and Heinonen 1980). Glutathione depletion in these cells was also reported (Xiong et al. 2021). Glutathione depletion has also been reported after *in vivo* exposure to acrolein (Arumugam et al. 1999a, 1999b; Lam et al. 1985; Struve et al. 2008). For example,

in rats exposed by inhalation, dose-related depletion of glutathione in the nasal respiratory and olfactory mucosa was seen after exposure to 0.1–3.6 ppm of acrolein for 1.5–3 hours (Lam et al. 1985; Struve et al. 2008).

Based on experimental results in rat liver and lung preparations (Patel et al. 1980) as well as *in vivo* studies in rats exposed by oral or i.v. administration (Parent et al. 1998) or subcutaneously (Kaye 1973), Stevens and Maier (2008) developed a metabolic scheme for acrolein (Figure 3-1). As shown in the figure, the major pathway begins with glutathione conjugation (either nonenzymatic or catalyzed by glutathione-S-transferase) in the liver. The glycine and gamma-glutamic acid residues are then enzymatically cleaved via cysteinylglycinase and gamma-glutamyl transferase (GGT), respectively, and the cysteine conjugate that results is metabolized by N-acetyl transferase to yield S-(3-oxopropyl) mercapturic acid (OPMA). OPMA may be reduced by aldo-keto reductase to 3-HPMA or oxidized via aldehyde dehydrogenase to CEMA. These reactions compete for the aldehydic site and result in the major and minor urinary metabolites, respectively. OPMA may also be oxidized by a flavin-containing monooxygenase (FMO) to yield OPMA-S-oxide, which can release acrolein to form sulfenic acid. Two minor pathways have also been proposed. The first involves the epoxidation of acrolein to glycidaldehyde and subsequent glutathione conjugation and conversion to N-acetyl-S-2-hydroxyethylcysteine, which is excreted in urine. Glycidaldehyde may also be metabolized to glyceraldehyde by epoxide hydrolase. In the second minor pathway, acrolein is metabolized by aldehyde dehydrogenase to acrylic acid which may subsequently converted to malonic acid.

Much of the information supporting the metabolic scheme presented above was based on toxicokinetic studies performed by Parent et al. (1996a, 1998) using male and female Sprague-Dawley rats exposed by gavage or i.v. administration to ^{14}C-acrolein. After a single i.v. or oral dose of 2.5 mg/kg, four and six metabolites (respectively) were identified, as shown in Table 3-1. The study authors suggested that the finding of significant quantities of oxalic acid (an oxidation product of malonic acid) after oral administration, but not i.v. administration, might be attributable to metabolism catalyzed by gut microbes (Parent et al. 1998).

Figure 3-1. Metabolism of Acrolein

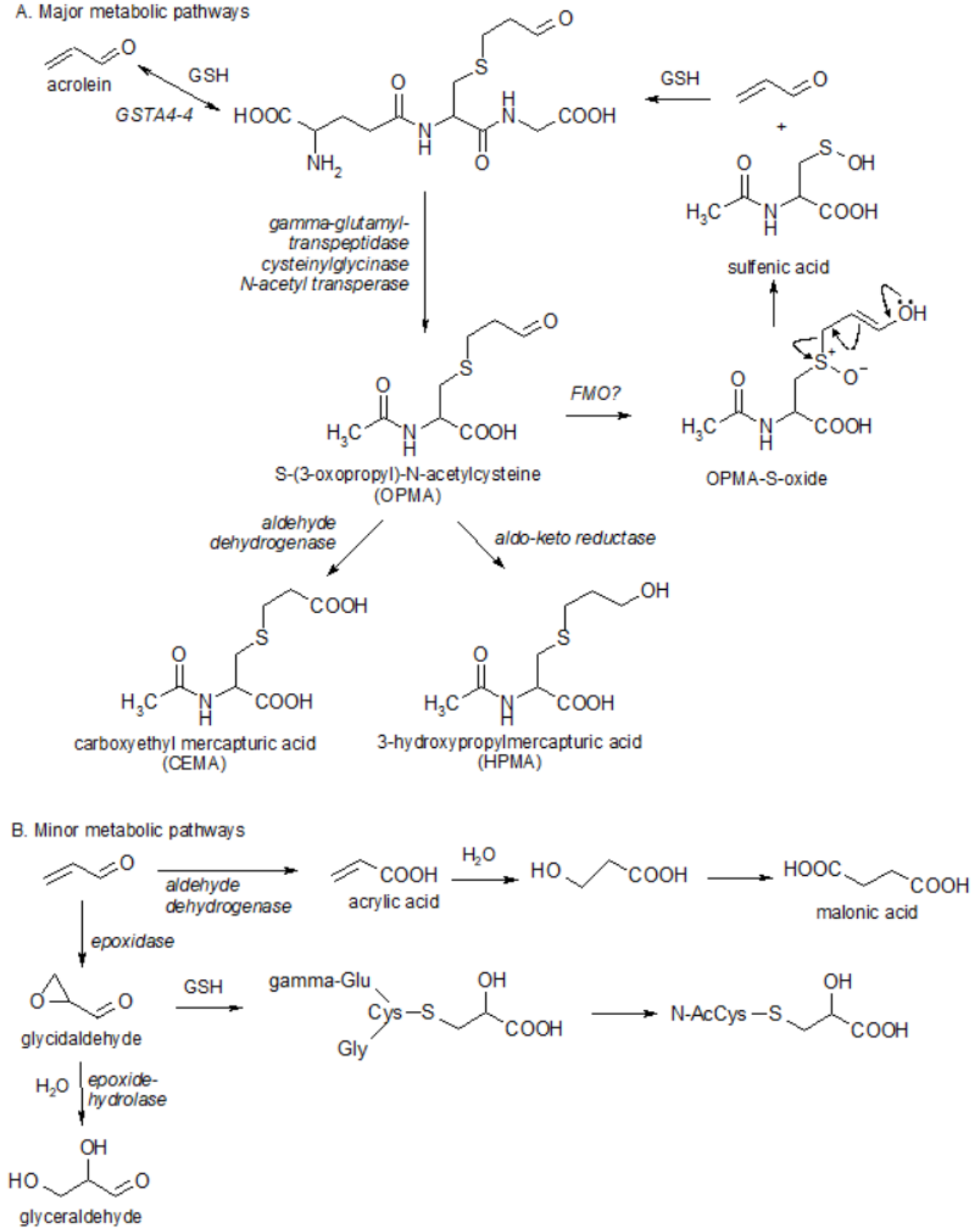

Source: Stevens and Maier (2008) © 2008 WILEY-VCH Verlag GmbH & Co. KGaA, Weinheim

Table 3-1. Metabolite Levels (Percent Sample Radioactivity) in Urine of Rats after Intravenous or Oral Dosing with 2.5 mg/kg Acrolein

	Intravenous (peak levels, 4–8 hours after dosing)[a]		Oral (peak levels, 0–4 hours after dosing)[a]	
Metabolite	Male	Female	Male	Female
3-HPMA	73.3%	74.4%	38.3%	41.2%
Oxalic acid	ND	ND	34.9%	32.9%
CEMA	5.6%	8.3%	11.7%	11.7%
N-Acetyl-S-2-carboxy-2-hydroxyethylcysteine	8.0%	5.5%	9.5%	7.8%
3-Hydroxypropionic acid	11.1%	10.8%	5.6%	6.5%
Malonic acid	ND	ND	Trace	Trace

[a]Values expressed as the percentage of initial sample radioactivity.

3-HPMA = 3-hydroxypropylmercapturic acid; CEMA = N-acetyl-S-(2-carboxyethyl)-L-cysteine; ND = not detected

Source: Parent et al. 1998

After both i.v. and oral dosing with 2.5 mg/kg acrolein, urinary excretion of metabolites was complete by 24 hours post dosing. Parent et al. (1998) exposed additional groups of animals to repeated oral doses of 2.5 mg/kg or a single dose of 15 mg/kg to evaluate the effects on metabolism. After a single high oral dose of 15 mg/kg, metabolites did not appear in the urine until 4–8 hours after dosing and continued to occur at measurable levels beyond 24 hours post dosing. The distribution of metabolites was similar after low and high oral doses as well as after repeated oral exposure (14 daily doses of unlabeled acrolein followed by a single dose of radiolabeled acrolein). In addition, there were no clear sex-related differences in metabolite distribution or excretion rates.

Studies in human smokers (Alwis et al. 2012; Carmella et al. 2007) and in animals (Alarcon 1976; Conklin et al. 2017b; Kaye 1973) support the identification of 3-HPMA as the major urinary metabolite of acrolein. Mice exposed to 0.5–1 ppm acrolein for 6 hours exhibited 2–3-fold increases in urinary levels of 3-HPMA (Conklin et al. 2017b). Similarly, 3-HPMA was identified in the urine of rats after a subcutaneous dose of acrolein (Alarcon 1976; Kaye 1973).

3.1.4 Excretion

No studies were located regarding excretion of acrolein or metabolites after inhalation or dermal exposure in humans or animals, or in humans after oral exposure.

The primary routes of acrolein excretion after oral and i.v. exposure are via urinary metabolites and exhaled carbon dioxide, with lesser amounts excreted in the feces. Available data suggest that urinary and fecal excretion after oral exposure is somewhat dose-dependent, and that there are no sex differences in excretory patterns. Parent et al. (1996a) found that in rats administered a dose of 2.5 mg/kg [2,3-^{14}C]acrolein via gavage, 30–31% of the initial dose was expired as CO_2, while 52–63% was found in the urine and 12–15% was found in the feces. Rats dosed with 15 mg/kg [2,3-^{14}C]acrolein exhibited similar expiration of the initial dose as CO_2, but had a higher fraction of the initial dose going to feces (28–31%) and a lower fraction going to urine (37–41%) (Parent et al. 1996a). Six metabolites of [2,3-^{14}C]acrolein were identified in the urinary fraction of the 2.5 mg/kg group: N-acetyl-S-2-carboxyethylcysteine; N-acetyl-S-2-hydropropylcysteine; N-acetyl-S-2-hydroxyethylcysteine; 3-hydroxypropionic acid; malonic acid; and oxalic acid (Parent et al. 1998). Analysis for metabolites in feces revealed no detectable metabolites. Draminski et al. (1983) reported the presence of the acrolein metabolite, S-carboxyethylmercapturic acid, in the urine of rats after administration of a single oral dose of 10 mg/kg of acrolein. The percentage of the dose recovered as the metabolite in the urine was not determined.

Rats administered 2.5 mg/kg [2,3-^{14}C]acrolein intravenously expired 26–27% of the initial dose as CO_2, which is lower, but not significantly different, from the amount expired by animals orally exposed to the same dose (Parent et al. 1996a). In this study, intravenously administered [2,3-^{14}C]acrolein was predominantly eliminated in the urine (67–69%), with a small fraction found in the feces (1–2%).

3.1.5 Physiologically Based Pharmacokinetic (PBPK)/Pharmacodynamic (PD) Models

Models are simplified representations of a system with the intent of reproducing or simulating its structure, function, and behavior. PBPK models are more firmly grounded in principles of biology and biochemistry. They use mathematical descriptions of the processes determining uptake and disposition of chemical substances as a function of their physicochemical, biochemical, and physiological characteristics (Andersen and Krishnan 1994; Clewell 1995; Mumtaz et al. 2012a; Sweeney and Gearhart 2020). PBPK models have been developed for both organic and inorganic pollutants (Ruiz et al. 2011) and are increasingly used in risk assessments, primarily to predict the concentration of potentially toxic moieties of a chemical that will be delivered to any given target tissue following various combinations of route, dose level, and test species (Mumtaz et al. 2012b; Ruiz et al. 2011; Sweeney and Gearhart 2020; Tan et al. 2020). PBPK models can also be used to more accurately extrapolate from animal to human,

high dose to low dose, route to route, and various exposure scenarios and to study pollutant mixtures (El-Masri et al. 2004). Physiologically based pharmacodynamic (PBPD) models use mathematical descriptions of the dose-response function to quantitatively describe the relationship between target tissue dose and toxic endpoints (Clewell 1995).

Research on PBPK models of acrolein have focused on simulating characteristics of the anatomy and physiology of the rodent and human respiratory tract that are thought to contribute to interspecies differences in dose-response relationships for nasal cavity lesions. Important features of acrolein toxicity and kinetics that are relevant to interspecies extrapolation include: (1) necrotic lesions of the nasal respiratory and olfactory epithelia (Dorman et al. 2008); (2) first-pass extraction of acrolein by nasal cavity tissues which decreases as the inhalation exposure concentration increases (Struve et al. 2008); and (3) saturable metabolic clearance of acrolein that contributes to dose-dependent extraction of acrolein in the respiratory tract (Patel et al. 1980; Struve et al. 2008).

Several models have been developed to simulate the kinetics uptake and metabolism of acrolein in the rodent and human respiratory tract (Asgharian et al. 2012; Schroeter et al. 2008; Xi et al. 2018). These models are described in detail in the following discussion because they provide a means to simulate the nasal cavity kinetics of acrolein in rats and humans for supporting interspecies dosimetry extrapolation (Schroeter et al. 2008).

Schroeter et al. (2008) Model

Description. Schroeter et al. (2008) developed a model to simulate the kinetics of inhaled acrolein in rats and humans. The core of the model is a computational fluid dynamics (CFD) model of the nasal cavity. The three-dimensional model was mapped to identify tissues representing the squamous epithelium, respiratory epithelium, and olfactory epithelium (see Figure 1 of Schroeter et al. 2008). Each tissue compartment is represented by layered sub-compartments that provide a diffusion pathway for acrolein in a surface mucus layer, epithelial layer, and submucosa. Inhaled acrolein deposits in the surface mucus layer and then diffuses to deeper sub-compartments where it is cleared by metabolism and absorption to blood. Transfer (flux, pg/cm^2 second) of acrolein from air to epithelial tissue is assumed to occur by diffusion, governed by the concentration in air at the mucus surface (pg/cm^3), an air-phase diffusion coefficient (cm^2/second), and a tissue/air partition coefficient. Exchanges between nasal tissue sub-compartments are also assumed to occur by diffusion governed by a diffusion coefficient and the concentration gradient between sub-compartments. Metabolism clearance of acrolein is simulated as a

first-order process (k, second^{-1}) combined with a saturable processes (V_{max}, K_M), with parameter values assigned to the epithelial and submucosal layers of squamous epithelium, respiratory epithelium, and olfactory epithelium. The disposition of metabolites is not simulated. Absorption to blood from the submucosal layer was simulated as a flow-limited sink with transfer governed by the concentration in the submucosal layer and blood flow to the submucosa.

Parameter Estimates and Calibration. Parameter values for rats and humans are presented in Tables 1 and 2 of Schroeter et al. (2008). Values for nasal cavity physiological parameters (air flow, blood flow, sub-compartment thickness) were adopted from previously published nasal cavity models (Bogdanffy et al. 1999; Frederick et al. 1998; Morris 1996; Morris et al. 1993; Plowchalk et al. 1997). The CFD models were constructed from magnetic resonance imaging of rat and human nasal cavities (Kimbell et al. 1997; Subramaniam et al. 1998). Air flow and air acrolein concentration in the nasal passages were calculated at approximately 150,000 locations (nodal points) in the three-dimensional model by solving a Navier-Stokes equation for a viscous incompressible fluid. An air-phase mass transfer coefficient was calculated at each nodal point assuming equilibrium conditions in which extraction from air was equal to uptake into tissue (Equations 1 and 2 from Schroeter et al. 2008). The air-phase mass transfer coefficient was calculated as the product of the diffusivity of acrolein in tissue (cm^2/second) and the tissue/air partition coefficient divided by the tissue depth. Values for the tissue-phase diffusion coefficient and tissue/air partition coefficient were based on values for formaldehyde measured in skin with adjustments for differences in the diffusivity of acrolein and formaldehyde in water and the water/air partition coefficients for the two chemicals (Kimbell et al. 2001; Loden 1986; RAIS 2023). Parameters for metabolism of acrolein in the nasal cavity of the rat were calibrated to achieve good fit to observations on nasal extraction of acrolein in rats (Morris 1996; Struve et al. 2008). The optimized value for the rat V_{max} was scaled to the human based on the human/rat ratio of the combined respiratory and olfactory surface areas (12.5). The rat value for the first-order metabolism rate coefficient was scaled to the human with a human/rat factor (0.4).

A sensitivity analysis of the model showed that predictions of the average flux of acrolein in olfactory tissues (used for interspecies dosimetry extrapolation) was most sensitive to changes in the metabolism V_{max}, the air/tissue partition coefficient and nasal tissue depth. Predictions showed low sensitivity to the values assigned the first-order metabolism rate coefficient, metabolism K_M, nasal blood flow, or mass transfer rates to the squamous epithelium.

Evaluation. After calibration of the metabolism parameters, the model predicted the overall dose-dependent and air flow-dependent nasal extraction fraction of acrolein in rats exposed to concentrations ranging from 1 to 9 ppm and flow rates ranging from 100 to 443 mL/minute (Morris 1996; Struve et al. 2008). In general, the predicted concentrations were within 20% of observations (shown in Figure 3 of Schroeter et al. 2008). Schroeter et al. (2008) did not report evaluations of the model against observations that were not included in calibrating model parameters.

Applications to Dosimetry. The model was used to predict regional nasal tissue acrolein doses from acrolein exposures in rats and humans (Schroeter et al. 2008). The model predicted a nonlinear decrease in the nasal extraction fraction over an exposure concentration range of 0.1–3.6 ppm. Nasal extraction fraction in the rat was predicted to be 2–3 times higher than in the human. The model predicted higher flux of acrolein into tissues in the anterior region of the nasal cavity compared to the posterior region, consistent with removal of acrolein from the inhaled air in the anterior region. Schroeter et al. (2008) predicted acrolein flux in respiratory and olfactory epithelia in regions of the nasal cavity where lesions were observed in rats exposed to 0.6–1.8 ppm (6 hours/day, 5 days/week) acrolein for periods of up to 65 days (Dorman et al. 2008). Consistent with higher incidences of nasal lesions at the 1.8 ppm exposure level, the model predicted higher tissue flux at the 1.8 ppm exposure level. In general, at the 1.8 ppm exposure level, higher tissue flux was predicted for regions of the nasal cavity that had higher lesion incidences.

Schroeter et al. (2008) applied the model to an interspecies dosimetry extrapolation of olfactory tissue lesions observed in the Dorman et al. (2008) study. Based on the Dorman et al. (2008) study, 0.6 and 1.9 ppm were identified as a NOAEL and LOAEL, respectively. The lowest flux predicted in olfactory tissues in nasal cavity regions that showed elevated lesion incidence (72 pg/cm^2 second) was used to represent the internal dose metric for the extrapolation to humans. This value was lower than the highest flux predicted for the NOAEL (191 pg/cm^2 second). The human model was used to predict fluxes at all nodal points in the olfactory regions of the human CFD model and the 99th percentile value was used to estimate the human equivalent concentration (HEC). The HEC was defined as the exposure that resulted in a 99th percentile flux in olfactory tissues equal to the rat internal dose metric (72 pg/cm^2 second). The HEC for continuous exposure was estimated to be 8 ppb.

Asgharian et al. (2012) Model

Description. Asgharian et al. (2012) developed a model to simulate the kinetics of reactive gases (acetaldehyde, acrolein, formaldehyde) in the human lung. The model simulates the uptake, metabolism, and absorption of acrolein at each airway generation (branching) number in a model of the thoracic and pulmonary regions of the human lung. The upper respiratory tract is not simulated. The model simulates the disposition of acrolein during the entire breathing cycle, which includes inhalation, pause, and exhalation phases. Inhaled acrolein deposits in the airway walls where it is cleared by metabolism and absorption to blood. Air flow in the lung is assumed to be uniform with the average laminar parabolic velocity. Transfer (flux, μg/cm^2 second) of acrolein from air to tissue is assumed to occur by diffusion, governed by the concentration in air at the mucus surface (pg/cm^3), an air-phase diffusion coefficient (cm^2/sec), and a tissue/air partition coefficient. A mass transfer coefficient (cm/second) that accounts for air phase and tissue phase mass transfer was calculated for the air-tissue equilibrium condition. Transfer within the tissue layer from airway wall to blood is assumed to occur by diffusion governed by a tissue-phase diffusion coefficient (cm^2/second), with the concentration at the tissue-blood interface assumed to be zero, reflecting complete clearance of acrolein by metabolism and absorption. Loss of acrolein vapor during the pause and exhalation phases of the breathing cycle is also simulated as a diffusion process governed by the air-phase diffusion coefficient and the concentration in air. Metabolism clearance of acrolein was simulated as a first-order process (k, second^{-1}) combined with a saturable process (V_{max}, K_M), and is assumed to occur in all regions of the lung. Disposition of metabolites is not simulated.

Parameter Estimates and Calibration. Parameter values for the acrolein model are presented in Table 1 of Asgharian et al. (2012). Values for the air-phase and tissue-phase diffusion coefficients, and metabolism parameters were from Schroeter et al. (2008). Airflow and concentrations of acrolein in each airway of the respiratory tract were estimated by solving a Navier-Stokes equation for a viscus incompressible fluid in a branching generation model of the human lung. Mass transfer coefficients were derived for the inhalation, pause, and exhalation phases of the breathing cycle (Asgharian et al. 2011). The concentration of acrolein in tissues was calculated from the reaction diffusion equation reported in Schroeter et al. (2008).

Asgharian et al. (2012) compared predictions from the formaldehyde model to predictions made with other reported models and with observations made during acetaldehyde exposures (Egle 1970; Overton et al. 2001). Evaluations of the acrolein model against observations were not reported.

Applications to Dosimetry. The model was used to predict regional airway (branching generation number) wall flux (rate of loss of acrolein from air to the airway walls) in the thoracic and pulmonary regions of human lung and tracheal tissue concentrations during inhalation of acrolein vapor (Asgharian et al. 2011). Flux was predicted to increase with increasing airflow, peaking at airway branch generations 8–10 when at rest (6.7/L minute) and at airway branch generations 17–18 during heavy exercise (55.3 L/minute). Acrolein concentrations in tracheal tissue were predicted to penetrate only to a depth of 80 µm and be higher at the end of the inspiratory phase of the breathing cycle compared to the end of the breathing cycle. The model predicted a nonlinear increase in tracheal tissue concentrations as the exposure concentration increased, consistent with a lack of strong reaction within the lung tissue, slow diffusion, and vapor release from the tissue back into the air stream (Asgharian et al. 2011, 2012).

Xi et al. (2018) Model

Description. Xi et al. (2018) developed a model to simulate the kinetics of acrolein in the respiratory tract of the rat. The model uses a CFD model of the respiratory tract that includes the nasal cavity, trachea, and lungs extending to the ninth airway bifurcation. The CFD model accounts for regions of turbulent and laminar air flow and deposition of acrolein aerosol droplets (see Figure 1 of Xi et al. 2018). Exposure was simulated as an aerosol of varying droplet diameters (0.48–8 nm) to simulate molecular aggregation of acrolein and water molecules. The tissue model includes two compartments representing the combined mucus and epithelial layer and a vascularized submucosa layer. Transfer (flux, pg/cm^2 second) of acrolein from air to epithelial tissue is assumed to occur by diffusion, governed by the concentration in air at the mucus surface (pg/cm^3), an air-phase mass transfer coefficient (cm/second), and a tissue/air partition coefficient. Acrolein in the epithelial layer is transferred to the submucosa where it is absorbed. Metabolism clearance of acrolein was simulated as a first order process (k, second^{-1}) combined with a saturable processes (V_{max}, K_M), with parameter values assigned to the epithelial and submucosal layers of squamous epithelium, respiratory epithelium, and olfactory epithelium. The disposition of metabolites is not simulated. The model assumes that acrolein that is not metabolized is completely absorbed to blood.

Parameter Estimates and Calibration. The CFD model was based on magnetic imaging of the lung of a 9–10-week-old Sprague-Dawley rat (Corley et al. 2012). A model of laminar and tubule flow in the rat respiratory tract was used to simulate air flow at 3.8 million nodal points of the CFD model (Kim et al. 2014; Li et al. 2017). The change in diameter of airway aerosol droplets resulting from molecular aggregation with water during passage through the airways was simulated using a molecular dynamic

model (Xi et al. 2018). Equations used to calculate transfer of acrolein to tissue were from previously reported models (Schroeter et al. 2008; Tian and Longest 2010a). Parameters for the two-layered model of the respiratory tract tissue were from Tian and Longest (2010a, 2010b). Parameters for diffusion and metabolism in respiratory tract tissue were from previously reported models (Schroeter et al. 2008; Tian and Longest 2010b).

Model predictions were compared to acrolein deposition fractions observed in rats (Struve et al. 2008). The model predicted that molecular aggregation contributed to a decrease in deposition fraction with increasing exposure concentration; however, it could not completely explain the observed decrease in deposition fraction, consistent with saturable metabolism being a major contributor.

Applications to Dosimetry. The model predicted a size dependence on regional deposition fractions, with the largest fraction deposited in the nose. Deposition in the nasal region decreased for approximately 75% for droplet sizes <1 nm to approximately 30% for 8-nm droplets. The size-dependent decrease in deposition in the nose resulted in a size-dependent increase in deposition in the trachea (see Figure 2 of Xi et al. 2018). Regional deposition was also found to be dependent on vapor diffusivity, with increasing deposition in the trachea relative to the nasal cavity, with decreasing diffusivity (see Figure 2 of Xi et al. 2018).

3.1.6 Animal-to-Human Extrapolations

The irritant properties of acrolein have been reported in both human and animal studies. *In vivo* studies in animals and *in vitro* studies in human and animal cell cultures have reported the common mechanisms of action of cellular thiol reactivity and glutathione depletion (Arumugam et al. 1999a, 1999b; Beauchamp et al. 1985; Nardini et al. 2002). Acrolein exposure levels were very comparable for the appearance of cellular changes in nasal epithelium of animals (Cassee et al. 1996a) and onset of nasal irritation in humans (Weber-Tschopp et al. 1977). Therefore, it is reasonable to extrapolate animal health effects to human health risk resulting from acrolein exposure.

3.2 CHILDREN AND OTHER POPULATIONS THAT ARE UNUSUALLY SUSCEPTIBLE

This section discusses potential health effects from exposures during the period from conception to maturity at 18 years of age in humans. Potential effects on offspring resulting from exposures of parental germ cells are considered, as well as any indirect effects on the fetus and neonate resulting from maternal

exposure during gestation and lactation. Children may be more or less susceptible than adults to health effects from exposure to hazardous substances and the relationship may change with developmental age.

This section also discusses unusually susceptible populations. A susceptible population may exhibit different or enhanced responses to certain chemicals than most persons exposed to the same level of these chemicals in the environment. Factors involved with increased susceptibility may include genetic makeup, age, health and nutritional status, and exposure to other toxic substances (e.g., cigarette smoke). These parameters can reduce detoxification or excretion or compromise organ function.

Populations at greater exposure risk to unusually high exposure levels to acrolein are discussed in Section 5.7, Populations with Potentially High Exposures.

Since point-of-contact irritation is the principal toxic action of acrolein, children are not likely to be more susceptible to acrolein's effects at the tissue level. Despite uncertainties in age-related differences in lung architecture, surface area, and ventilation rates, simple dosimetry modeling of a category 1 gas, such as acrolein, does not suggest significant differences in early juvenile and adult internal inhalation exposure (Ginsberg et al. 2005). It is not known if there are age-related differences in the pharmacokinetics of acrolein. The amount of ingested acrolein available for gastrointestinal irritation would be the same for children and adults. While children may have a higher inhalation rate (per mass) than adults (NRC 1993), it is unknown whether they would continue to breathe more airborne acrolein than adults. While adults have been shown to reduce their respiration rate by as much as 20% in the presence of airborne acrolein (Weber-Tschopp et al. 1977), it is not known if children will react in the same or similar manner. Animal studies have shown offspring of acrolein-exposed mothers to have reduced body weights and skeletal deformities (EPA 1983; Parent et al. 1992c). However, these effects occurred at high oral doses that were fatal to the mothers.

In general, individuals whose respiratory function is compromised, such as those with emphysema, or individuals with allergic airway disease such as rhinitis and/or allergic asthma, will be at a higher risk of developing adverse respiratory responses when exposed to a strong respiratory irritant such as acrolein. This was demonstrated in animals in which allergic airway-diseased mice were more responsive than non-diseased mice to acute respiratory irritant effects of 0.3 ppm acrolein (Morris et al. 2003).

3.3 BIOMARKERS OF EXPOSURE AND EFFECT

Biomarkers are broadly defined as indicators signaling events in biologic systems or samples. They have been classified as biomarkers of exposure, biomarkers of effect, and biomarkers of susceptibility (NAS/NRC 2006).

The National Report on Human Exposure to Environmental Chemicals provides an ongoing assessment of the exposure of a generalizable sample of the U.S. population to environmental chemicals using biomonitoring (see http://www.cdc.gov/exposurereport/). If available, biomonitoring data for acrolein from this report are discussed in Section 5.6, General Population Exposure.

A biomarker of exposure is a xenobiotic substance or its metabolite(s) or the product of an interaction between a xenobiotic agent and some target molecule(s) or cell(s) that is measured within a compartment of an organism (NAS/NRC 2006). The preferred biomarkers of exposure are generally the substance itself, substance-specific metabolites in readily obtainable body fluid(s), or excreta. Biomarkers of exposure to acrolein are discussed in Section 3.3.1.

Biomarkers of effect are defined as any measurable biochemical, physiologic, or other alteration within an organism that (depending on magnitude) can be recognized as an established or potential health impairment or disease (NAS/NRC 2006). This definition encompasses biochemical or cellular signals of tissue dysfunction (e.g., increased liver enzyme activity or pathologic changes in female genital epithelial cells), as well as physiologic signs of dysfunction such as increased blood pressure or decreased lung capacity. Note that these markers are not often substance specific. They also may not be directly adverse, but can indicate potential health impairment (e.g., DNA adducts). Biomarkers of effect caused by acrolein are discussed in Section 3.3.2.

A biomarker of susceptibility is an indicator of an inherent or acquired limitation of an organism's ability to respond to the challenge of exposure to a specific xenobiotic substance. It can be an intrinsic genetic or other characteristic or a preexisting disease that results in an increase in absorbed dose, a decrease in the biologically effective dose, or a target tissue response. If biomarkers of susceptibility exist, they are discussed in Section 3.2, Children and Other Populations that are Unusually Susceptible.

3.3.1 Biomarkers of Exposure

Identification of a specific and reliable biomarker of acrolein exposure has proven to be challenging. As discussed in Section 3.1, acrolein is produced endogenously during various biological process (e.g., lipid peroxidation). None of the proposed biomarkers of exposure can distinguish between endogenous and exogenous sources of acrolein exposure.

Urinary excretion of 3-HPMA and CEMA, products of the conjugation of acrolein with glutathione, have been proposed as biomarkers of acrolein exposure. However, neither metabolite is a specific biomarker for acrolein exposure. Several other compounds are also metabolized to 3-HPMA, including allylamine (Boor et al. 1987), allyl halides (Kaye and Young 1972), and allyl alcohol, allyl formate, allyl nitrate, and allyl propionate (Kaye 1973). 3-HPMA is also a proposed biomarker to monitor the toxicity of the chemotherapy drug, cyclophosphamide, which generates 3-HPMA via a metabolic pathway that produces acrolein (Harahap et al. 2020). Acrylonitrile is also metabolized into CEMA, and urinary CEMA is a proposed biomarker for acrylonitrile exposure (Jakubowski et al. 1987; Luo et al. 2020; Wu et al. 2023). Initial reports in small groups of volunteers (n=6) suggested poor correlation between respiratory uptake of inhaled acrylonitrile and urinary CEMA levels, indicating that CEMA may not be a reliable index of acrylonitrile exposure (Jakubowski et al. 1987); however, subsequent studies in larger groups (n=79) showed significant correlation between airborne acrylonitrile levels and urinary CEMA levels following occupational exposure (Wu et al. 2023). Since both acrylonitrile and acrolein are found in cigarette smoke, and smoking is a major exposure route for the general population for both acrolein (Section 5.6) and acrylonitrile (Wu et al. 2023), CEMA produced from the metabolism of acrylonitrile may confound findings of studies that use CEMA as a biomarker of acrolein exposure.

Alwis et al. (2012) developed a method to examine urinary metabolites of VOCs, including 3-HPMA and CEMA as specific metabolites of acrolein. To validate the method, they compared urinary levels of 3-HPMA and CEMA in smokers and nonsmokers. Higher 3-HPMA and CEMA levels were detected in the urine of tobacco smokers, and there was a significant correlation between these urinary metabolites and serum cotinine (a biomarker for tobacco intake), supporting the use of 3-HPMA and CEMA as markers of exposure to acrolein (Alwis et al. 2012). Chen et al. (2019) evaluated the stability of urinary levels of 3-HPMA as a biomarker of acrolein exposure from cigarette smoke. Urine samples were collected over the course of 20 weeks from a group of smokers supplied with research cigarettes (Chen et al. 2019). The results indicated that 3-HPMA excretion was “fairly” stable in smokers (with steady intake) by repeated measures correlation. The longitudinal consistency intra-class correlation coefficient (ICC) for 3-HPMA

was 0.46. The "fair" performance of this metabolite was attributed to the fact that acrolein exposure from sources other than cigarette smoke was likely to have affected the correlation.

Data in animals also show a relationship between acrolein exposure and urinary 3-HPMA. In mice, exposure to 0.5 or 1 ppm acrolein for 6 hours resulted in 2–3-fold increases in urinary levels of creatinine-adjusted 3-HPMA (Conklin et al. 2017a). Zheng et al. (2013) showed that when rats were injected (intraperitoneal or intraspinal) with acrolein, urinary levels of 3-HPMA were elevated in a dose-dependent manner. This effect was inhibited when rats were co-administered acrolein scavengers (hydralazine or phenelzine), supporting the supposition that 3-HPMA in the urine was a specific biomarker for acrolein and correlated with exposure.

Recently, a method was developed for measuring acrolein concentrations in serum (Imazato et al. 2015). In the study, acrolein in serum from humans with no known exposure was measured at levels ranging from 2.2 to 5.15 μM. As with urinary metabolite levels, serum measurements of acrolein do not provide a method for differentiation between endogenous and exogenous acrolein.

3.3.2 Biomarkers of Effect

Available biomarkers of acrolein effects cannot distinguish between exogenous and endogenous acrolein sources. Acrolein interacts with DNA to form mutagenic adducts including the exocyclic acrolein-deoxyguanosine adduct, AdG (Chen and Lin 2009; Liu et al. 2005). It has been proposed that these adducts could be used as specific biomarkers of DNA damage induced by acrolein (Chen and Lin 2011). Methods to detect these specific adducts in human saliva (Chen and Lin 2011), placenta (Chen and Lin 2009), and human lymphocytes (Chen and Lin 2009; Yin et al. 2013) have been developed. In addition, Wang et al. (2019) observed increased buccal cell acrolein-DNA adducts in humans up to 24 hours after they consumed fried fast foods (a known source of acrolein exposure).

Acrolein-lysine adducts have been proposed for use as urinary and plasma biomarkers of oxidative stress/oxidative damage (Chen et al. 2022b; Chen 2023; Moghe et al. 2015). It is important to note, however, that these acrolein adducts have also been proposed as biomarkers for a wide variety of disease states ranging from Alzheimer's disease (Yoshida et al. 2023) to osteoporosis (Herr et al. 2021).

3.4 INTERACTIONS WITH OTHER CHEMICALS

Acrolein inhalation was shown to alter the uptake of acetone from the upper respiratory tract of rats and mice under co-exposure conditions (Morris 1996; Morris et al. 2003). Acrolein exposure produced an increase in the uptake of acetone (up to 2-fold) and prevented acetone from achieving steady-state absorption (Morris 1996; Morris et al. 2003).

Ansari et al. (1988) showed that acrolein enhances the inhibitory effect that certain industrial chemicals, such as styrene and 1,2-dichloroethane, have on the α-l-proteinase inhibitor of human plasma *in vitro*. A decrease in the activity of the α-l-proteinase inhibitor may result in an increase in the activity of the lung enzyme neutrophil elastase, which can lead to the development of emphysema.

Acrolein has been shown to increase the pentobarbital- and hexobarbital-induced sleeping time in rats (Jaeger and Murphy 1973). The mechanism, according to the study authors, could include changes in the absorption and distribution of the barbiturates. The mechanism may involve a covalent reaction between acrolein and cytochrome P450, leading to inactivation of P450 and prolonged action of the barbiturates (Lame and Segall 1987).

Acrolein forms adducts with thiols such as glutathione, cysteine, N-acetylcysteine, and others. These reactions protect tissues and cells from the cytotoxic effects of acrolein or acrolein-releasing substances (Brock et al. 1981; Chaviano et al. 1985; Dawson et al. 1984; Gurtoo et al. 1981; Ohno and Ormstad 1985; Whitehouse and Beck 1975). However, at higher acrolein exposure levels, depletion of glutathione renders tissues susceptible to damage from other endogenous and exogenous sources of oxidative stress.

Exposure of mice for 10 minutes to mixtures of sulfur dioxide and acrolein showed that either irritant can alter or block the effect of the other (Kane and Alarie 1979). Furthermore, when the mice were exposed to mixtures, recovery was much slower than when exposed to the individual chemicals. The study authors postulated that a bisulfite-acrolein adduct may be formed. When exposure ceased, this adduct would release acrolein, thus preventing immediate recovery.

Kane and Alarie (1978) exposed mice to mixtures of acrolein and formaldehyde and showed that the respiratory response to mixtures was less pronounced than the response to either chemical alone. However, *in vitro* studies using human bronchial epithelial BEAS-2B cells demonstrated that co-exposure to formaldehyde and acrolein resulted in synergistic effects on cytotoxicity and measures of oxidative

stress (Zhang et al. 2019), apoptosis (Zhang et al. 2020b), and DNA damage (Zhang et al. 2020a, 2020b). Similarly, Zhang et al. (2018) reported synergistic effects of formaldehyde and acrolein on measures of cytotoxicity, DNA damage, and micronuclei in human lung carcinoma A549 cells.

Human subjects exposed to side-stream smoke containing acrolein reported a higher degree of annoyance than a different group of subjects exposed to the same concentration of acrolein alone, suggesting that other smoke constituents contribute to irritant effects (Weber-Tschopp et al. 1977).